CHAPTER 2

EXPERIMENTAL SETUP AND METHODOLOGY

2.1 Introduction

As observed in Chapter 1, all the properties of conventional lead-tin solders were discussed, along with the difficulties arising from the presence of lead in the environment and its impact on human health. Additionally, various types of calorimeters were discussed, alongside the challenges associated with the use of lead-free solder. Within this chapter, the typical purity, sources, chemical compositions, and other pertinent details of the principal elements of all raw materials are listed. Furthermore, a comprehensive detailing of the specifications of the MHTC 96 LINE EVO high temperature drop calorimeter from SETARAM, France, is provided. The experimental procedure for calorimetric measurements of enthalpy is thoroughly discussed. Various interpolation geometrical models, namely Kohler, Muggianu, Chou, Toop, and Hillert, are also discussed upon, and a comparison of our experimental data with data predicted from these models is conducted and plots will be discussed in next chapters. The confidence in and reliability of the data are substantially boostered, as the quantities are experimentally measured and cross-referenced with data predicted from geometrical interpolation models and by the CALPHAD method. A good agreement between experimental and predicted data is observed.

2.2 Materials

In order to study the thermodynamic behavior, drop calorimetric study of binary and ternary alloys were done by using pure metals. The specifications for pure metals and protective Argon gas are listed in **Table 2.1**. As a standard for calibration, α-Al_2O_3 needles from the NIST (National Institute of Standards and Technology) in Gaithersburg, Maryland, United States were used. Here, α-Al_2O_3 needles were used because the enthalpy values of these needles are known. After being cleaned with n-hexane in a supersonic bath, metals were vacuum-dried in an antechamber glove box to remove any trace of the solvent that may have been left behind. All metals were initially in solid form. After that, they were cut up into smaller pieces and weighed to an accuracy of 10^{-4} g by using Sartorius balance type Cubis. A vacuum pumping system (Hind High Vacuum, India Model: VS 114PD) was used to generate vacuum.

Table 2.1 Purity, Sources and Physical state of Materials.

Material	Purity (%)	Supplier	Physical state
Indium	99.999	JM, UK	**Rod**
Tin	99.999	JM, UK	**Shots**
Gallium	99.999	JM, UK	**Ingot**
Antimony	99.999	JM, UK	**Ingot**
Bismuth	99.999	JM, UK	**Ingot**
Argon	99.999 (vol %)	IOL,INDIA	**Gas**

JM = Johnson Matthey

IOL = Indian Oxygen Limited, India

2.3 MHTC 96 LINE EVO high temperature drop calorimeter from SETARAM, France

It is a type of drop calorimeter consisting of a thermopile which is a cluster of 56 thermocouples (see **Figure 2.1**). Graphite tube resistance furnace of this calorimeter operates up to working temperature of 1593 K. An automatic dropping device (Multi-sample Introducer) is used for the dropping of the sample from the top of the calorimeter. There is a provision of fixing the time interval in the multi sample introducer for the dropping of 23 samples (maximum). There is an alumina tube that connects the furnace to the dropping device to guide the sample. Sample is dropped from automatic sample introducer to the crucible (placed in the furnace) by this tube. Furnace and crucible chambers are degassed by a vacuum pump connected to the instrument.

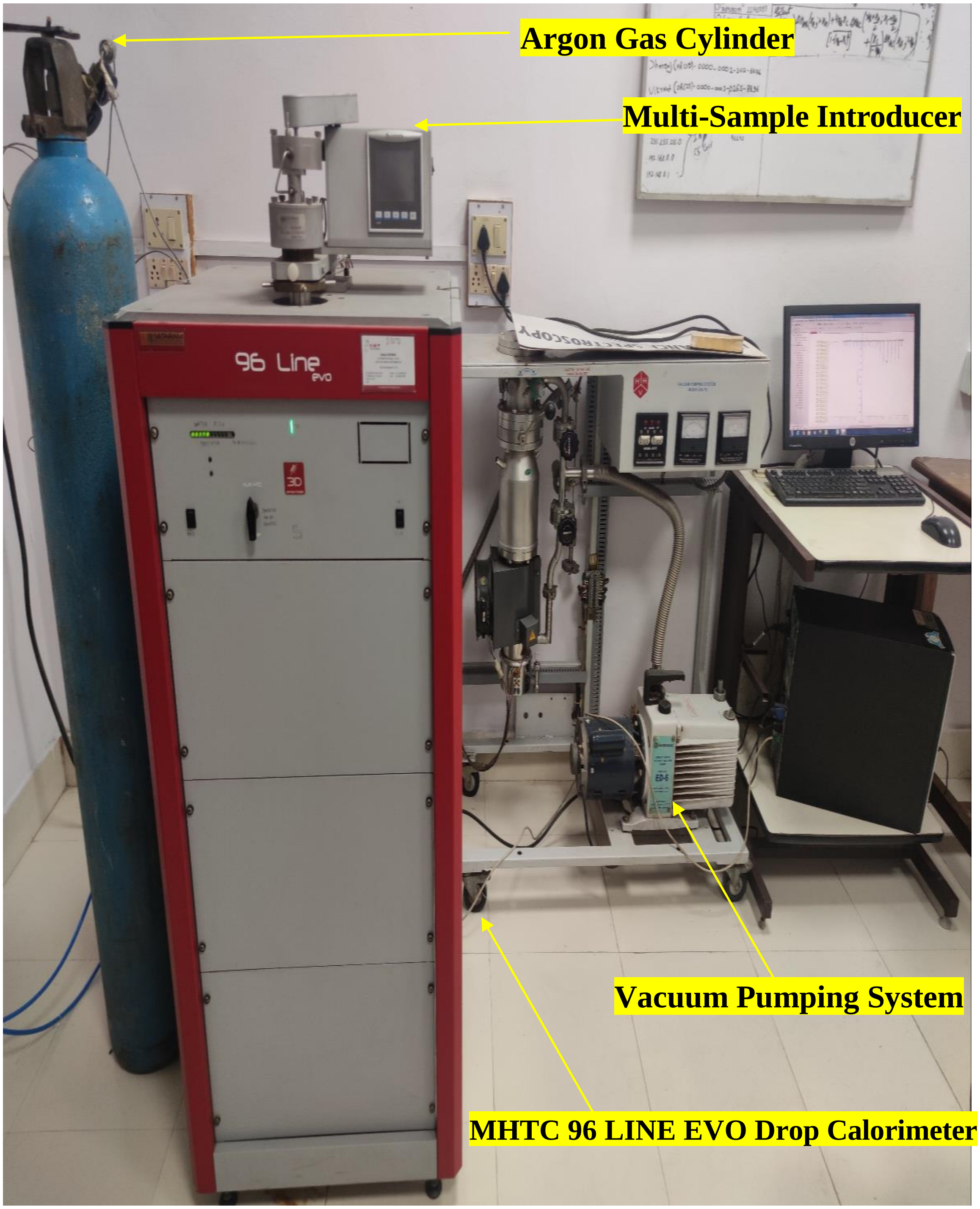

Fig. 2.1 MHTC 96 LINE EVO High Temperature Drop Calorimeter with all accessories.

The experiment is conducted in a flowing argon gas atmosphere to avoid oxidation of the samples. Control of process parameters during the experiment is done by Calisto Data Acquisition Software and analysis of the peaks is done by Calisto Data Processing Software supplied by the manufacturer.

MHTC 96 LINE EVO high temperature drop calorimeter consists of the following parts:

2.3.1 Motorized lifting device

This part lifts up the thermos gravimetric transducer so as to reach the experimenting crucibles.

2.3.2 Multi-Sample Introducer

This is an automatic dropping device (Multi-sample introducer) used for dropping multiple samples one after another in a fixed interval of time. This device (see **Figure 2.2**) can drop 23 samples into the crucible into controlled atmosphere at a fixed interval of time. It is necessary that each sample can fit inside a 1 mm to 5mm diameter sphere. The samples are loaded in a fluid-tight barrel linked to the crucible via the drop tube. The operator is then free to drop the samples automatically by fixing time interval between each drop. Multi-Sample Introducer comprises of:

i. A 23-sample introducer.

ii. An electronic unit with a digital screen, motor, belt transmission system and a protective cover.

iii. A template for adjusting the transmission belt tension.

iv. A 24V power supply module mounted in the rack.

v. A 24V power cable for the electronic unit.

Fig. 2.2 Multi-Sample Introducer

2.3.3 High temperature furnace

This is a cylindrical furnace hung from the cabinet’s top plate. Schematic representation of high temperature furnace section is shown in **Figure 2.3**. The heating element (1), fitted in the center-line, is a graphite tube with its tapered end embedded in the cylindrical shaped copper contact, current intakes (2) (3) are fitted to the furnace by insulated bolts (4) and elastic washers (5). This arrangement makes possible expansion of the resistor. A graphite-felt sleeve (6) limits the resistor’s heat loss. A sealed alumina tube (7) crosses the furnace through the center of the heating element. It forms the experimenting chamber and enables insulation between the furnace's atmosphere and that of the experimenting chamber. This tube (7) is held at the top by the furnace's nose (8) and at the bottom by the lower mounting plate (9), which has O-rings (10) for sealing. The furnace bottom is blanked off by the lower flange (11) supporting the Temperature-control thermocouple (17) and the screening facility (18). Connected to this flange are the lower union for the sweeping gas inlet (14), the union for the vacuum pump (15) on the experimenting chamber and connector for the Temperature-control thermocouple (16).

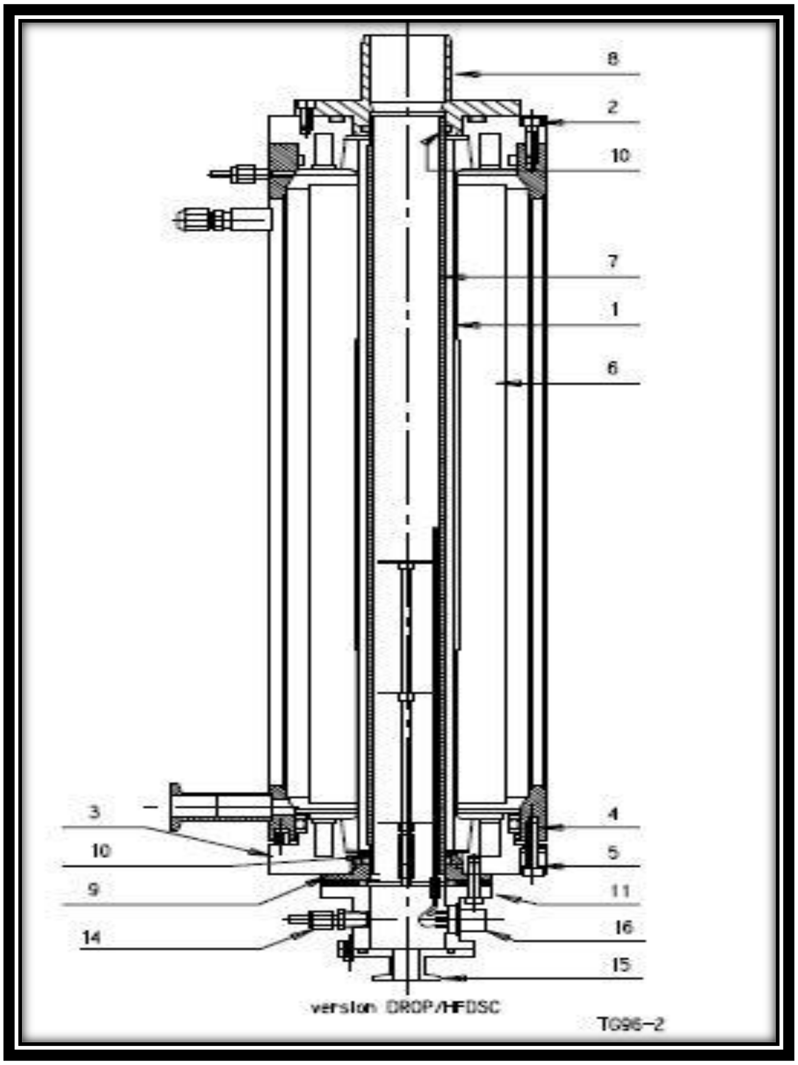

Fig. 2.3 Schematic representation of High temperature furnace section.

2.3.4 Degassing unit

Argon gas was introduced into the furnace working area at a pressure of 3.5 bar for a duration of 12 hours. This step aimed to purge any residual gases and create an inert atmosphere within the furnace. Following the argon sweeping, the furnace underwent a series of heating cycles. Each cycle consisted of ramping the temperature from 20°C to 500°C at a rate of 10°C per minute. Argon sweeping was applied during these cycles to maintain the inert atmosphere within the furnace. A minimum of five heating cycles were performed with the application of argon sweeping. This ensured thorough conditioning of the furnace and stabilization of its temperature profile. Upon completion of the heating cycles with argon sweeping, the furnace was deemed ready for operation. The accumulated cycles helped to establish consistent thermal conditions within the furnace, essential for subsequent experimental procedures.

2.3.5 Drop tube

The basic version is equipped with an alumina drop tube having two functions:

- **i.** Guiding the sample during the drop or mixing experiment.
- **ii.** Exhausting corrosive vapors potentially given off by the sample.

2.3.6 Crucibles

Alumina drop tube guides the samples from fluid tight barrel to the crucible. The drop calorimeter is equipped with cylindrical alumina crucibles having the following inner dimensions: **Diameter =** 13 mm**, Height =** 40 mm**, Volume =** 5.3 cm^3 (working volume). Do not exceed a filling height of 30 mm, so as to avoid any overflowing of the samples mixture. According to the samples, the choice is done between:

- ❖ Either an alumina crucible

- Or an alumina crucible with its platinum-lining.

2.3.7 Software evolution controller

This central unit is integrated in the structure of the 96 LINE EVO device, is composed of several electronic modules:

2.3.7.1 CPU module

This module runs the programming and temperature control for the thermal analyzer through the power module, according to the sequences set by the user. The acquisition and digitizing of the various signals (temperature, DTA/DSC, TMA signal) takes place. The transfer of the digitalized signals to a computer via an Ethernet interface.

2.3.7.2 Temperature acquisition modules

These modules execute the conditioning and the acquisition of two temperature signals (furnace temperature and sample temperature) via two thermocouples.

2.3.7.3 Gas panel module

It runs the opening or closing of the electro-valves on the gas panel, namely those of the Carrier Gases 1, 2 and 3, the Auxiliary Gas, the Protective Gas, purging and mixing of Auxiliary Gas with one of the Carrier Gases. The two mass flow rate regulators on the carrier gas and auxiliary gas circuits. It measures the pressure inside the analysis chamber and the flow rates of the Carrier and Auxiliary Gases.

2.3.7.4 Controller modules part

This unit is composed of:

i. The command module which controls the furnace and the electro-valves 230.
ii. The box of the temperature control thermocouple.
iii. The sample temperature measurement coming from the sensor head.

iv. The low level amplifier module of DTA or DSC signals.

v. The gravimetric analysis function.

2.3.8 Rear Power rack part

It contains:

i. The controller supply.

ii. The CPU board with an Ethernet connection and the CAN connection which is sent inside the instrument through a cable.

iii. The general power supply inlet controlled by the circuit breaker.

iv. The mains supply redistribution for the peripheral functions (electro-valves, vacuum gauge, TMA box, gas control board, and controller).

v. The power control and its security function, ensured by means of the card.

2.4 Calorimetric technique and procedure

Drop calorimetric technique has been successfully used for the measurement of the enthalpy of formation of binary, ternary and higher order alloys.

2.4.1 Experimental Procedure

2.4.1.1 Starting up the instrument

Calorimeter is started by switching on power. The switch is located on back side of the calorimeter. Inlet gas pressure is maintained around 1 to 1.15 bar. Water tap is turned on for cooling.

2.4.1.2 Starting up the Calisto software

The Computer is switched on and then waited for 5 minutes. Calisto software is started by clicking data acquisition icon on the desktop. Program experiment or MHTC96 CS Evolution window is opened by clicking window tab in the top menu.

2.4.1.3 Programming the experiment

A new experiment is selected by clicking program experiments window. In right side a new experiment is created (see **Figure 2.4**). In Experiment Properties tab, name of the experiment is changed, type of crucible is selected and mass of the sample is entered. In the procedure tab, settings like experiment group, end / pause mode are selected. In procedure properties sample and furnace temperature, carrier gas and safety temperatures are selected. By right clicking on the experiment name, three standard zones are created (Heating zone, Isothermal zone and Cooling zone). By clicking on serial no. tab sequences are added to the standard zones. During first zone (heating zone), furnace is heated at a given rate of 5 K/min to the desired temperature and samples are melted down in crucible. During second zone (isothermal zone), furnace is maintained at constant temperature and samples are dropped into the crucible. The time between each drop is generally 35 to 40 minutes. Extra time of 180 minutes is provided for stabilization in the starting of isothermal zone and 20 minutes after last drop for complete melting and mixing. In third zone (cooling zone), furnace is cooled to room temperature at a given rate. In this zone, 10 minutes are given after cooling for stabilization and after that gas flow, water flow are closed.

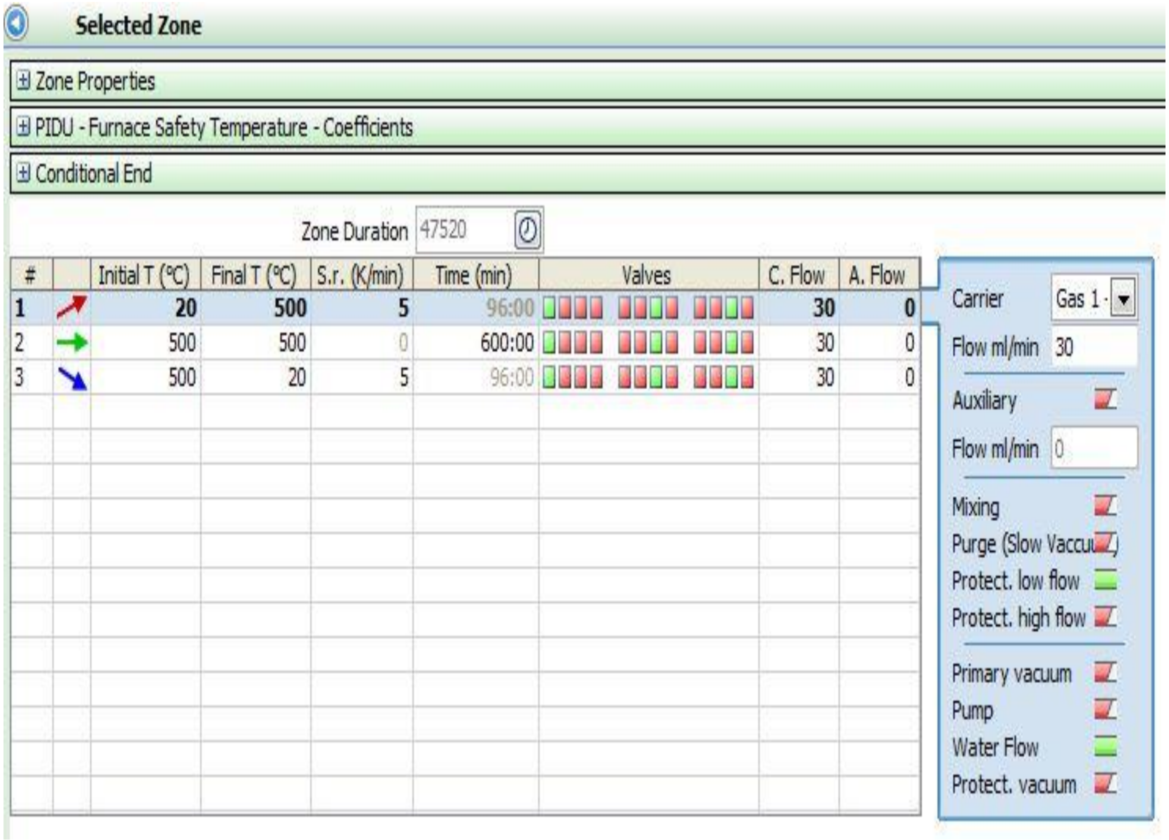

Selected Zone

⊞ Zone Properties

⊞ PIDU - Furnace Safety Temperature - Coefficients

⊞ Conditional End

Zone Duration 47520

#		Initial T (°C)	Final T (°C)	S.r. (K/min)	Time (min)	Valves	C. Flow	A. Flow
1	↗	**20**	**500**	**5**	96:00	🟩🟥🟥🟥 🟥🟥🟩🟥 🟥🟥🟩🟥	**30**	**0**
2	→	500	500	0	600:00	🟩🟥🟥🟥 🟥🟥🟩🟥 🟥🟥🟩🟥	30	0
3	↘	500	20	5	96:00	🟩🟥🟥🟥 🟥🟥🟩🟥 🟥🟥🟩🟥	30	0

Carrier	Gas 1
Flow ml/min	30
Auxiliary	🟥
Flow ml/min	0
Mixing	🟥
Purge (Slow Vaccu	🟥
Protect. low flow	🟩
Protect. high flow	🟥
Primary vacuum	🟥
Pump	🟥
Water Flow	🟩
Protect. vacuum	🟥

Fig. 2.4 Experiment Programming

2.4.1.4 Sample Loading

Samples are loaded into alumina crucible by lifting up the dropping tube by pressing the Black button on the front left side of the calorimeter. Again by pressing the button dropping tube is moved down. Samples to be dropped are loaded into the Multi-Sample introducer. Time interval of 40 min is set between each drop.

2.4.1.5 Starting the experiment

After everything is ready the experiment is started by clicking start button under window tab. After finishing the experiment, the files are opened in Calisto processing software and area of each peak is measured.

2.4.1.6 Area measurement

After finishing the experiment, the files are opened in Calisto processing software. The area of each peak is measured using baseline integration option under math tab. Starting and end points of the peaks are selected for measuring area of individual peaks.

2.4.1.7 Necessity of calibration

The aim is to calibrate the transducer so as to transform the electrical signal $\Delta\boldsymbol{H}_{\boldsymbol{signal}}$ (in microvolts sec) into energy (in Joule) by the help of calibration constant K. The heat signal ($\Delta\boldsymbol{H}_{\boldsymbol{Signal}}$) value associated with the α-Al_2O_3 needle drops served as the basis for determining the calibration constant (K) and by using NIST standard data for α-Al_2O_3 needle we got $\Delta\boldsymbol{H}_{\boldsymbol{alumina}}$ values for the given temperature change. The coefficient of calibration K is then determined as:

$$\mathbf{K} = \frac{\Delta\boldsymbol{H}_{\boldsymbol{alumina}}}{\Delta\boldsymbol{H}_{\boldsymbol{Signal}}} \tag{2.1}$$

This coefficient of calibration K varies with various parameters:

- The sample shape and mass.
- The properties of the transducer.
- The experimenting temperature.
- The properties of the crucible.
- The properties and flow-rate of the sweeping gas.

So, four samples of α-Al_2O_3 is dropped at the end of each run so as to obtain the calibration constant at that particular flow rate, temperature and pressure.

2.4.1.8 Enthalpy calculations

After being multiplied by the calibration constant K, the integral values of each heat signal were then converted to enthalpy that we call it as heat effect. Calculating the enthalpy, or heat effect, for each given heat signal requires the multiplication of the integral values of that signal by a known value of calibration constant (K). Here, the reaction enthalpy **($\Delta\boldsymbol{H}_{\boldsymbol{Reaction,X,i}}$)** which is a function of heat effect ***($\Delta\boldsymbol{H}_{\boldsymbol{Signal,X,i}} \cdot \boldsymbol{K}$)*** and the enthalpy **($\Delta\boldsymbol{H}_{\boldsymbol{X,i}}^{\boldsymbol{T_D}\rightarrow\boldsymbol{T_M}}$)** increment of the sample to be dropped, is calculated by **Equation 2.2** when species $\boldsymbol{X}$ is dropped from drop temperature **($\boldsymbol{T_D}$)** to bath temperature **($\boldsymbol{T_M}$)**.

$$\Delta\boldsymbol{H}_{\boldsymbol{Reaction,X,i}} = (\Delta\boldsymbol{H}_{\boldsymbol{Signal,X,i}} \cdot \boldsymbol{K}) \; - (\Delta\boldsymbol{H}_{\boldsymbol{X,i}}^{\boldsymbol{T_D}\rightarrow\boldsymbol{T_M}} \cdot \boldsymbol{n}_{\boldsymbol{X,i}}) \tag{2.2}$$

Where $\boldsymbol{n}_{\boldsymbol{X,i}}$ (no. of moles) is the number of species $\boldsymbol{X}$ that was dropped into the liquid bath with the help of an automated dropping system, and each peak is associated with a distinct $\Delta\boldsymbol{H}_{\boldsymbol{Signal,X,i}}$ value, which is the integrated area (in µVs). It was computed using baseline integration tool for every peak. The change in the molar enthalpy of species $\boldsymbol{X}$ is represented by $\Delta\boldsymbol{H}_{\boldsymbol{X,i}}^{\boldsymbol{T_D}\rightarrow\boldsymbol{T_M}}$ and may be evaluated with the use of enthalpy data found in the literature [98] for each species within the appropriate temperature range.

Although a very small amount of species $\boldsymbol{X}$ was added in with the liquid metal in the crucible, **Equation 2.3** may be used to calculate the **partial enthalpy $\Delta\overline{\boldsymbol{H}}_{\boldsymbol{X,i}}$:**

$$\Delta\overline{\boldsymbol{H}}_{\boldsymbol{X,i}} \approx \; \Delta\boldsymbol{H}_{\boldsymbol{Reaction,X,i}}/\boldsymbol{n}_{\boldsymbol{X,i}} \tag{2.3}$$

For **Ga-In, Ga-Sn** and **In-Sn** binary alloy systems during each measurement included carefully putting predetermined quantities of one of the two metals into the crucible, followed by the controlled introduction of the other metals at the designated temperature.

Depending on the various binary systems, pieces of pure Indium were dropped into molten Gallium which is kept in crucible in the case of Ga-In system and; Tin into molten Gallium and Tin into molten Indium in the case of Ga-Sn and In-Sn binary systems, respectively. **Equation 2.4** gives the **integral molar mixing enthalpy (**$\Delta \boldsymbol{H}_{\boldsymbol{mix}}$**)** as follows:

$$\Delta \boldsymbol{H}_{\boldsymbol{mix}} = \frac{\sum \Delta \boldsymbol{H}_{\boldsymbol{Reaction}}}{(\boldsymbol{n}_{\boldsymbol{crucible}} + \sum \boldsymbol{n}_{\boldsymbol{i}})} \qquad \textbf{(2.4)}$$

For **Sn-Ga-In** ternary system during each measurement, two of the three metals were added to the crucible in precise proportions before the third was added at the designated temperature. Pieces of pure tin were dropped into molten $Ga_{0.25}In_{0.75}$, $Ga_{0.50}In_{0.50}$, $Ga_{0.75}In_{0.25}$ alloys and pieces of pure Indium into $Ga_{0.25}Sn_{0.75}$, $Ga_{0.50}Sn_{0.50}$, $Ga_{0.75}Sn_{0.25}$.

For **Sn-Bi-Sb** ternary system, Bi was placed into the crucible and Sb was then dropped and then Sn were dropped in the binary Bi-Sb; Sb was placed into the crucible and Sn was then dropped and then Bi were dropped in the binary Sb-Sn; and Sn was placed into the crucible and Bi was then dropped and then Sb were dropped in the binary Bi-Sn.

The integral molar mixing enthalpy ($\Delta \boldsymbol{H}_{\boldsymbol{mix}}$) of ternary system can be calculated by using **Equation 2.5**.

$$\Delta \boldsymbol{H}_{\boldsymbol{mix}} = \frac{(\boldsymbol{n}_{\boldsymbol{binary}}) * (\Delta_{\boldsymbol{mix}} \boldsymbol{H}_{\boldsymbol{respective\ binary}}) + \sum \Delta \boldsymbol{H}_{\boldsymbol{Reaction}}}{(\boldsymbol{n}_{\boldsymbol{binary}} + \sum \boldsymbol{n}_{\boldsymbol{X,i}})} \qquad \textbf{(2.5)}$$

Here $\boldsymbol{n}_{\boldsymbol{binary}}$ = total no. of moles of two base metals in crucible

$\Delta_{\boldsymbol{mix}} \boldsymbol{H}_{\boldsymbol{respective\ binary}}$= enthalpy of mixing value for the initial composition of binary in the crucible.

2.5 Geometric modelling

Five extrapolation geometric models (Kohler, Muggianu, Chou, Toop and Hillert) were used to predict the enthalpy of mixing values of ternary Sn-Ga-In and Sn-Bi-Sb systems. Binary interaction parameter of all binaries were required to predict the thermodynamic properties of the given ternary system. Binary interaction parameter of all binary systems In-Sn, Ga-In ,Ga-Sn, Bi-Sb, Sb-Sn, and Bi-Sn were taken from the data available in literature [130], [140].

The various predictive extensions from the binary to ternary **i-j-k** System (see **Figures 2.5-2.9**) are shown below:

2.5.1 Kohler model [141], [142]

$$\Delta \boldsymbol{H}^{\boldsymbol{mix}}_{\boldsymbol{i-j-k}} = \Big[(\boldsymbol{x_i} + \boldsymbol{x_j})^{\boldsymbol{2}} \Delta \boldsymbol{H}^{\boldsymbol{mix}}_{\boldsymbol{i-j}} \left(\frac{\boldsymbol{x_i}}{\boldsymbol{x_i} + \boldsymbol{x_j}}; \frac{\boldsymbol{x_j}}{\boldsymbol{x_i} + \boldsymbol{x_j}} \right) + (\boldsymbol{x_j} + \boldsymbol{x_k})^{\boldsymbol{2}} \Delta \boldsymbol{H}^{\boldsymbol{mix}}_{\boldsymbol{j-k}} \left(\frac{\boldsymbol{x_j}}{\boldsymbol{x_j} + \boldsymbol{x_k}}; \frac{\boldsymbol{x_k}}{\boldsymbol{x_j} + \boldsymbol{x_k}} \right) +$$

$$(\boldsymbol{x_k} + \boldsymbol{x_i})^{\boldsymbol{2}} \Delta \boldsymbol{H}^{\boldsymbol{mix}}_{\boldsymbol{k-i}} \left(\frac{\boldsymbol{x_k}}{\boldsymbol{x_k} + \boldsymbol{x_i}}; \frac{\boldsymbol{x_i}}{\boldsymbol{x_k} + \boldsymbol{x_i}} \right) \Big] \qquad \textbf{(2.6)}$$

2.5.2 Muggianu model [141], [142]

$$\Delta \boldsymbol{H}^{\boldsymbol{mix}}_{\boldsymbol{i-j-k}} = \Bigg[\left(\frac{\boldsymbol{4x_i x_j}}{[\boldsymbol{1} - (\boldsymbol{x_i} - \boldsymbol{x_j})^{\boldsymbol{2}}]} \right) \Delta \boldsymbol{H}^{\boldsymbol{mix}}_{\boldsymbol{i-j}} \left(\boldsymbol{x_i} + \frac{\boldsymbol{x_k}}{\boldsymbol{2}}; \boldsymbol{x_j} + \frac{\boldsymbol{x_k}}{\boldsymbol{2}} \right) +$$

$$\left(\frac{\boldsymbol{4x_j x_k}}{[\boldsymbol{1} - (\boldsymbol{x_j} - \boldsymbol{x_k})^{\boldsymbol{2}}]} \right) \Delta \boldsymbol{H}^{\boldsymbol{mix}}_{\boldsymbol{j-k}} \left(\boldsymbol{x_j} + \frac{\boldsymbol{x_i}}{\boldsymbol{2}}; \boldsymbol{x_k} + \frac{\boldsymbol{x_i}}{\boldsymbol{2}} \right) + \left(\frac{\boldsymbol{4x_k x_i}}{[\boldsymbol{1} - (\boldsymbol{x_k} - \boldsymbol{x_i})^{\boldsymbol{2}}]} \right) \Delta \boldsymbol{H}^{\boldsymbol{mix}}_{\boldsymbol{k-i}} \left(\boldsymbol{x_k} + \frac{\boldsymbol{x_j}}{\boldsymbol{2}}; \boldsymbol{x_i} + \frac{\boldsymbol{x_j}}{\boldsymbol{2}} \right) \Bigg]$$

…… … ……… …2.7)

2.5.3 Chou model [141], [142]

$$\Delta \boldsymbol{H}^{\boldsymbol{mix}}_{\boldsymbol{i-j-k}} = \Big[\left(\frac{\boldsymbol{x_j}}{\boldsymbol{1} - \boldsymbol{x_i}} \right) \Delta \boldsymbol{H}^{\boldsymbol{mix}}_{\boldsymbol{i-j}} (\boldsymbol{x_i}; \boldsymbol{x_j}) + \left(\frac{\boldsymbol{x_k}}{\boldsymbol{1} - \boldsymbol{x_j}} \right) \Delta \boldsymbol{H}^{\boldsymbol{mix}}_{\boldsymbol{j-k}} (\boldsymbol{x_j}; \boldsymbol{x_k}) +$$

$$\left(\frac{\boldsymbol{x_i}}{\boldsymbol{1} - \boldsymbol{x_k}} \right) \Delta \boldsymbol{H}^{\boldsymbol{mix}}_{\boldsymbol{k-i}} (\boldsymbol{x_k}; \boldsymbol{x_i}) \Big] \qquad \textbf{(2.8)}$$

2.5.4 Toop model [141], [142]

$$\Delta \boldsymbol{H}^{\boldsymbol{mix}}_{\boldsymbol{i-j-k}} = \Big[\left(\frac{\boldsymbol{x_j}}{\boldsymbol{1} - \boldsymbol{x_i}} \right) \Delta \boldsymbol{H}^{\boldsymbol{mix}}_{\boldsymbol{i-j}} (\boldsymbol{x_i}; \boldsymbol{1} - \boldsymbol{x_i}) + (\boldsymbol{x_j} + \boldsymbol{x_k})^{\boldsymbol{2}} \Delta \boldsymbol{H}^{\boldsymbol{mix}}_{\boldsymbol{j-k}} \left(\frac{\boldsymbol{x_j}}{\boldsymbol{x_j} + \boldsymbol{x_k}}; \frac{\boldsymbol{x_k}}{\boldsymbol{x_j} + \boldsymbol{x_k}} \right) +$$

$$\left(\frac{\boldsymbol{x_k}}{\boldsymbol{1} - \boldsymbol{x_i}} \right) \Delta \boldsymbol{H}^{\boldsymbol{mix}}_{\boldsymbol{k-i}} (\boldsymbol{x_i}; \boldsymbol{1} - \boldsymbol{x_i}) \Big] \qquad \textbf{(2.9)}$$

2.5.5 Hillert model [141], [142]

$$\Delta \boldsymbol{H}^{mix}_{i-j-k} = \left[\left(\frac{x_j}{1-x_i}\right)\Delta \boldsymbol{H}^{mix}_{i-j}(\boldsymbol{x_i}; \boldsymbol{1} - \boldsymbol{x_i}) + \left(\frac{4x_j x_k}{[1-(x_j-x_k)^2]}\right)\Delta \boldsymbol{H}^{mix}_{j-k}\left(\boldsymbol{x_j} + \frac{x_i}{2}; \boldsymbol{x_k} + \frac{x_i}{2}\right) + \left(\frac{x_k}{1-x_i}\right)\Delta \boldsymbol{H}^{mix}_{k-i}(\boldsymbol{x_i}; \boldsymbol{1} - \boldsymbol{x_i})\right] \quad (2.10)$$

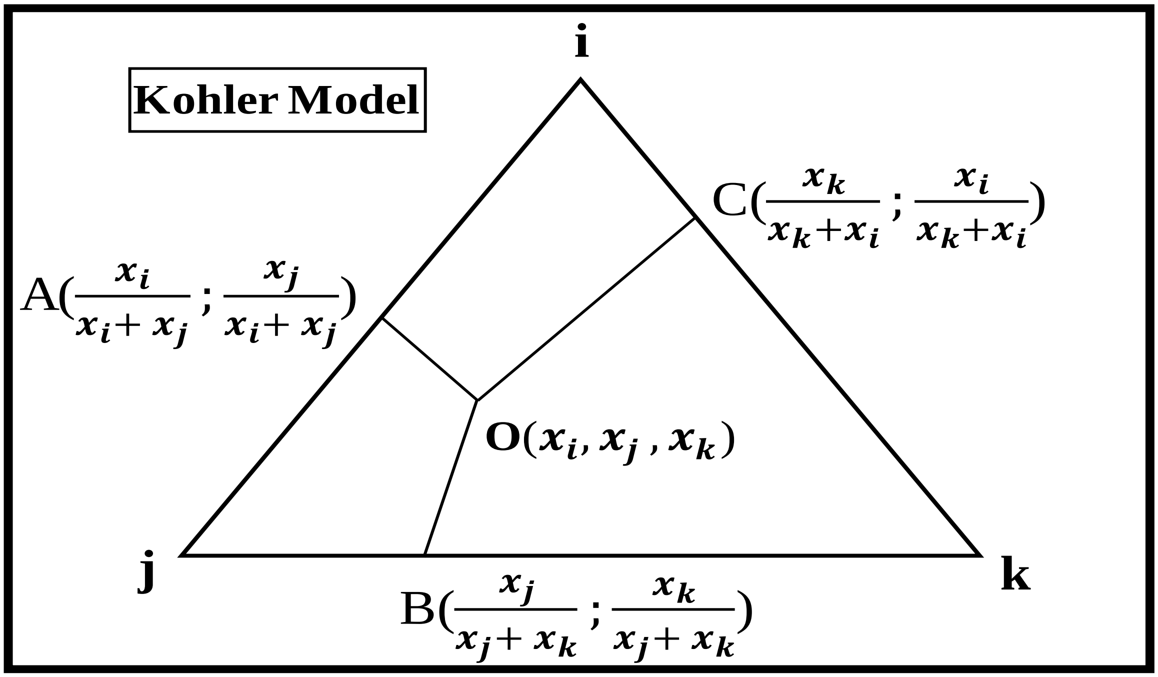

Fig. 2.5 Geometrical path followed by kohler model.

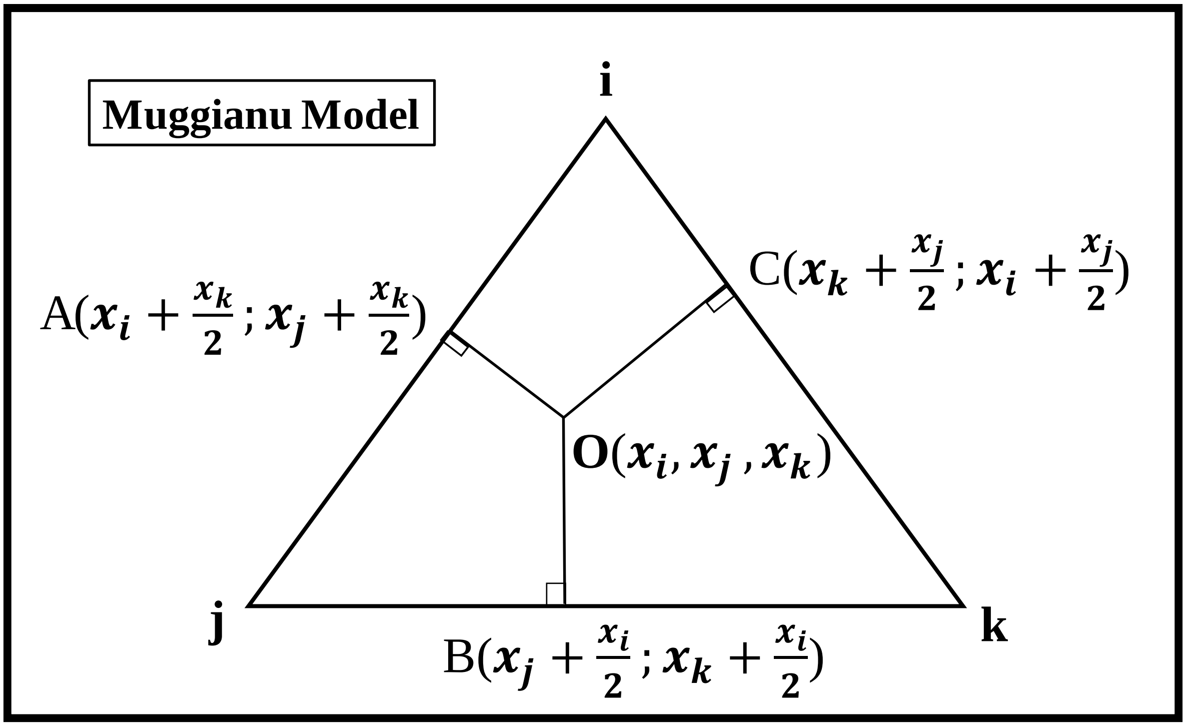

Fig. 2.6 Geometrical path followed by Muggianu model.

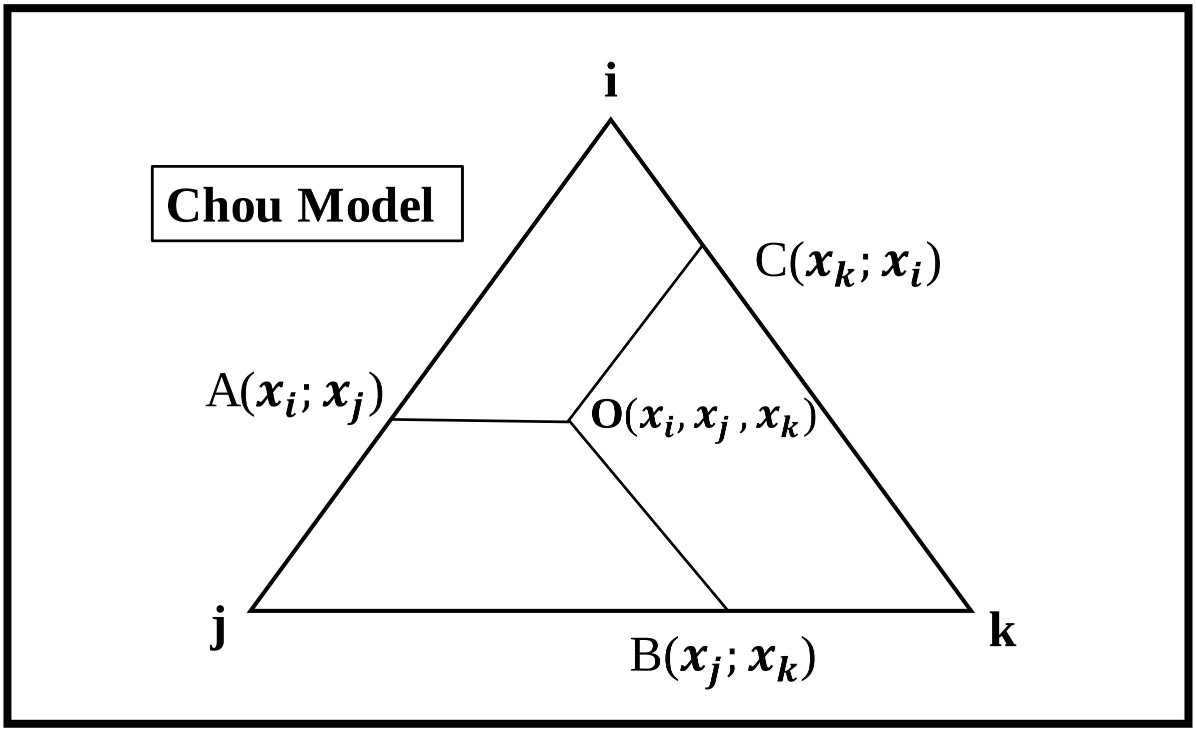

Fig. 2.7 Geometrical path followed by Chou model.

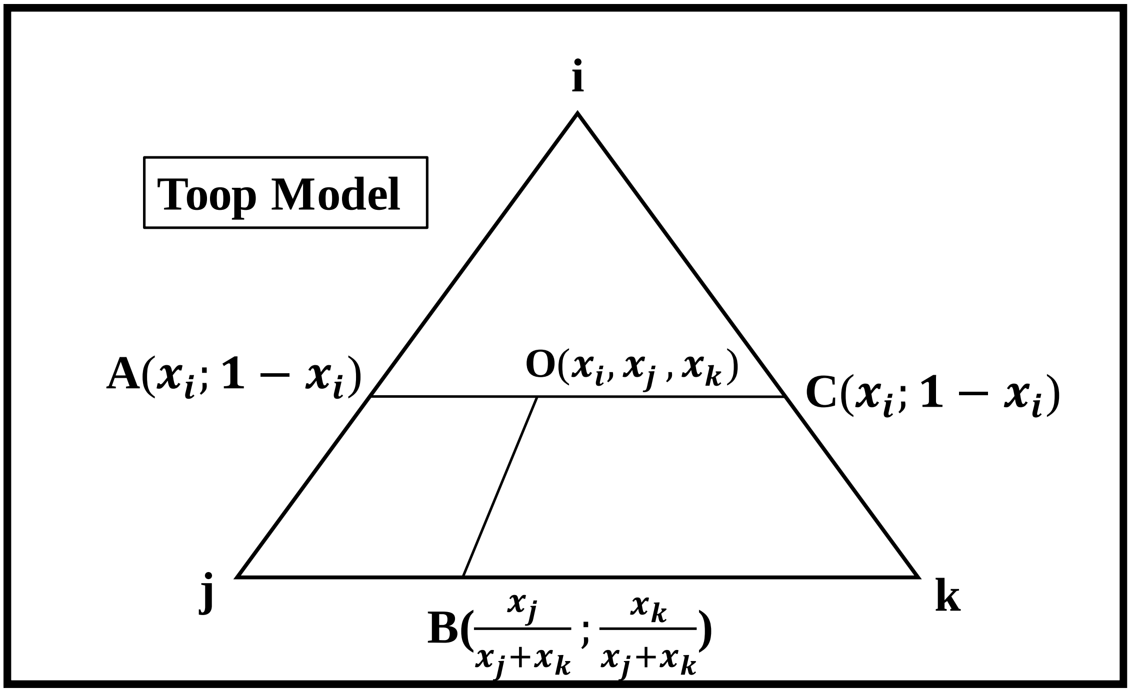

Fig. 2.8 Geometrical path followed by Toop model.

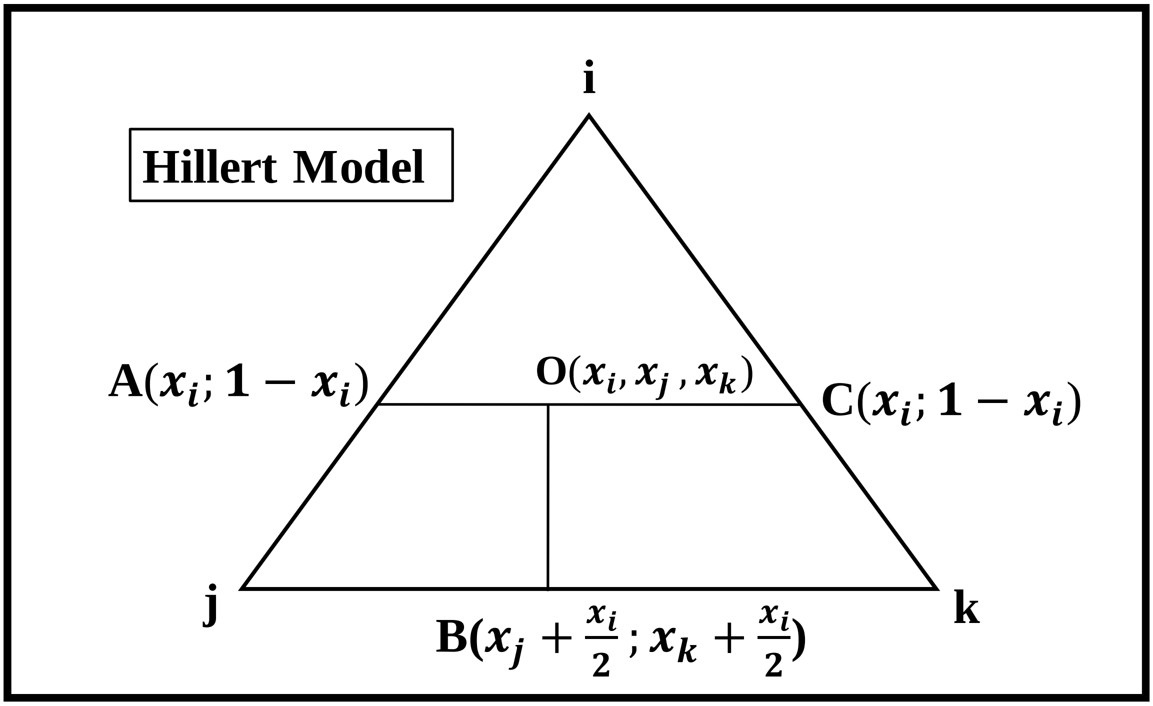

Fig. 2.9 Geometrical path followed by Hillert model.

2.6 Redlich Kister Muggianu (RKM) Polynomial Modelling Equation

2.6.1 For Binary Systems

For substitutional solutions, Ansara and Dupin [143] offer the following Redlich-Kister polynomial, which was used to fit the experimental calorimetric data for the enthalpies of mixing of all the binaries at different temperatures. The data set was fitted using least squares fit in accordance with **Equation 2.11**.

$$\Delta \boldsymbol{H_{mix}} = \sum_i \sum_{j>i} \left[\boldsymbol{x_i x_j} \sum_v \boldsymbol{L_{i:j}^{(v)}} \left(\boldsymbol{x_i} - \boldsymbol{x_j} \right)^{\boldsymbol{v}} \right] \qquad \textbf{(2.11)}$$

where $L_{i:j}^{(v)}$(ν= 0, 1, 2, **…**) are the interaction parameters(binary) of the binary systems.

2.6.2 For Ternary System

Luef et al. [127] have also used the Redlich-Kister-Muggianu polynomial for substitutional solutions. To determine the ternary interaction parameters, we performed a least-squares fit to the available data using **Equation 2.12**.

$$\Delta \boldsymbol{H_{mix}} = \sum_i \sum_{j>i} \left[\boldsymbol{x_i x_j} \sum_v \boldsymbol{L_{i:j}^{(v)}} \left(\boldsymbol{x_i} - \boldsymbol{x_j} \right)^{\boldsymbol{v}} \right] + \boldsymbol{x_i x_j x_k} (\boldsymbol{L_{i:j:k}^{0}} \, \boldsymbol{x_i} + \boldsymbol{L_{i:j:k}^{1}} \, \boldsymbol{x_j} + \boldsymbol{L_{i:j:k}^{2}} \, \boldsymbol{x_k}) \ldots\ldots \textbf{(2.12)}$$

where $\boldsymbol{L_{i:j}^{(v)}}$(**ν**= 0, 1, 2, …) are the interaction parameters(binary) of the binary systems and $\boldsymbol{L_{i:j:k}^{\nu}}$ (ν= 0, 1, 2,…) are the interaction parameters(ternary). The experimentally determined mixing enthalpy is then compared with the estimated values, with just the binary contributions being taken into consideration.

2.7 Iso-Enthalpy plots

These plots are called iso-enthalpy plots because the enthalpy value remains constant along these curves regardless of variations in composition. To generate these plots, the values of molar mixing enthalpy with respect to the amount of the species that is to be dropped are used. Different curves are obtained for different enthalpy values. These plots help in determining the optimal composition where the alloy will be most stable.

2.8 CALPHAD Method

The CALPHAD method, an acronym derived from "Calculation of Phase Diagrams," is a computational approach widely used in materials science and metallurgy to predict and analyze phase equilibria in multicomponent systems. This method integrates principles from thermodynamics, computational science, and materials engineering to model the complex interactions between different phases and components in materials. The CALPHAD method represents a powerful framework for understanding and predicting the behavior of materials in complex multicomponent systems. Its combination of thermodynamic principles, computational techniques, and experimental data makes it an indispensable tool for materials scientists and engineers seeking to design and optimize materials for a wide range of technological applications.